Electronic Supplementary Material (ESI) for Physical Chemistry Chemical Physics


# Supporting Information

## Computational modeling of single- versus double-anchoring modes in di-branched organic sensitizers on $TiO_2$ surfaces: structural and electronic properties

Joaquín Calbo,[a] Mariachiara Pastore,[b,*] Edoardo Mosconi,[b] Enrique Ortí,[a,*] Filippo De Angelis[b,*]

[a]*Instituto de Ciencia Molecular, Universidad de Valencia, 46980 Paterna, Spain*
[b]*Computational Laboratory for Hybrid Organic Photovoltaics (CLHYO), Istituto CNR di Scienze e Tecnologie Molecolari, via Elce di Sotto 8, I-06123, Perugia, Italy. Fax + 39 075 585 5606 Tel. +39 075 585 5522.*

E-mail: chiara@thch.unipg.it, enrique.orti@uv.es, filippo@thch.unipg.it

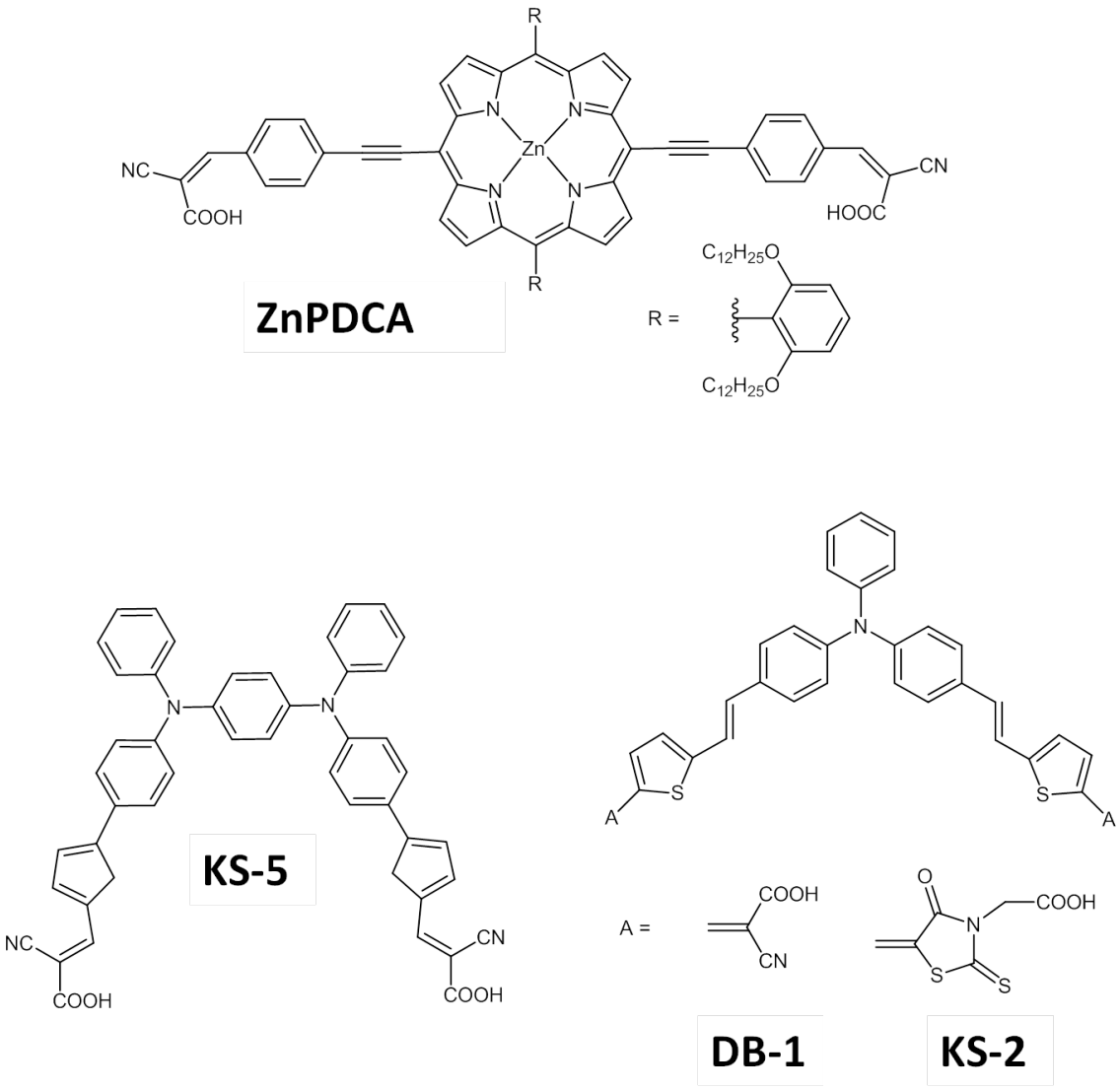


**Scheme S1**. Chemical structure of several donor-π-acceptor di-branched dyes used in dye-sensitized solar cells.

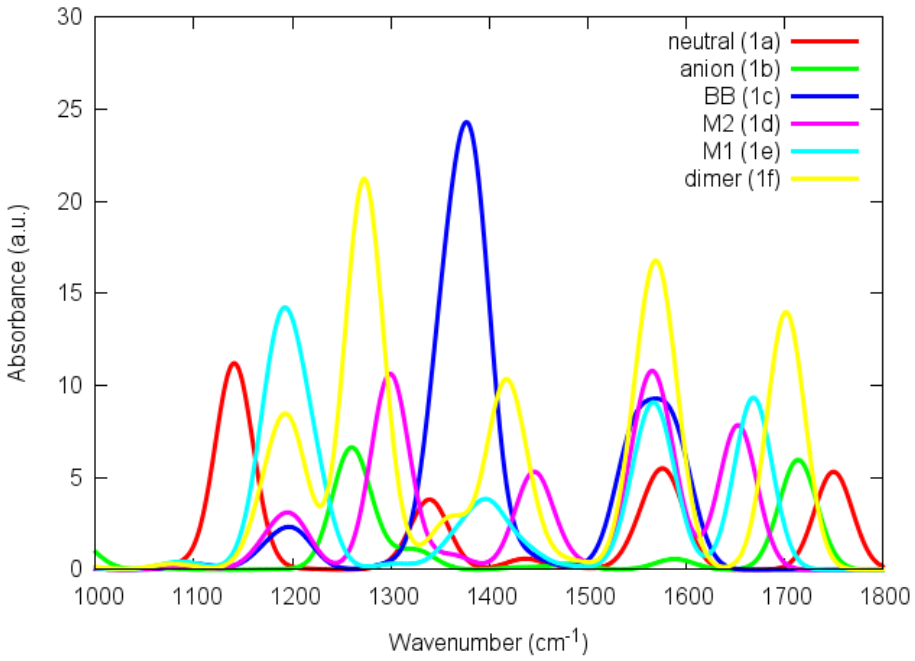


**Figure S1**. IR spectra computed at B3LYP/6-31G* in gas phase for system **1** in all anchoring environments modeled (structures **1a-1f** in Figure 4).

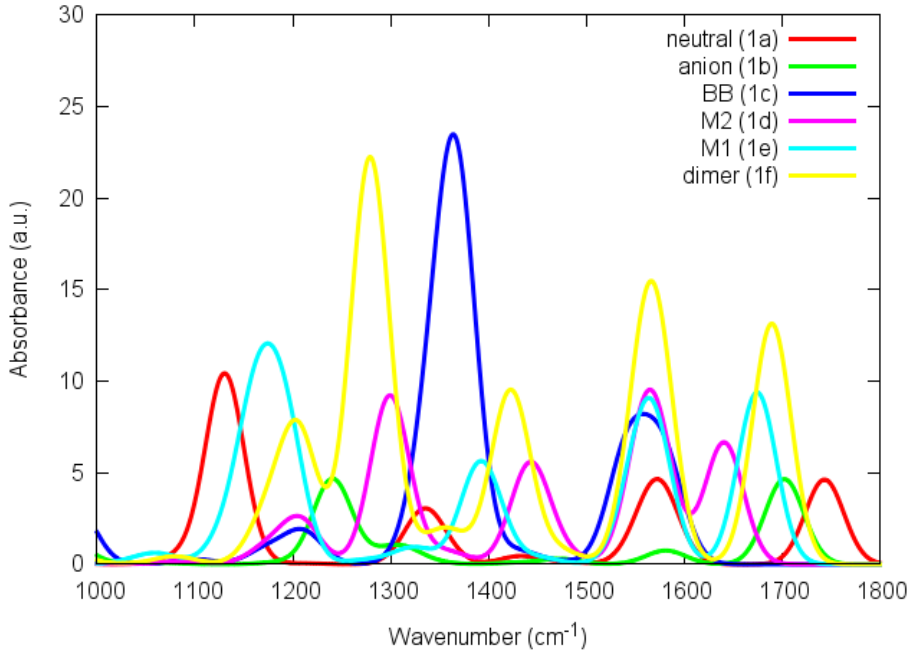


**Figure S2**. IR spectra computed at PBE0/6-31G* in gas phase for system **1** in all anchoring environments modeled (structures **1a-1f** in Figure 4).

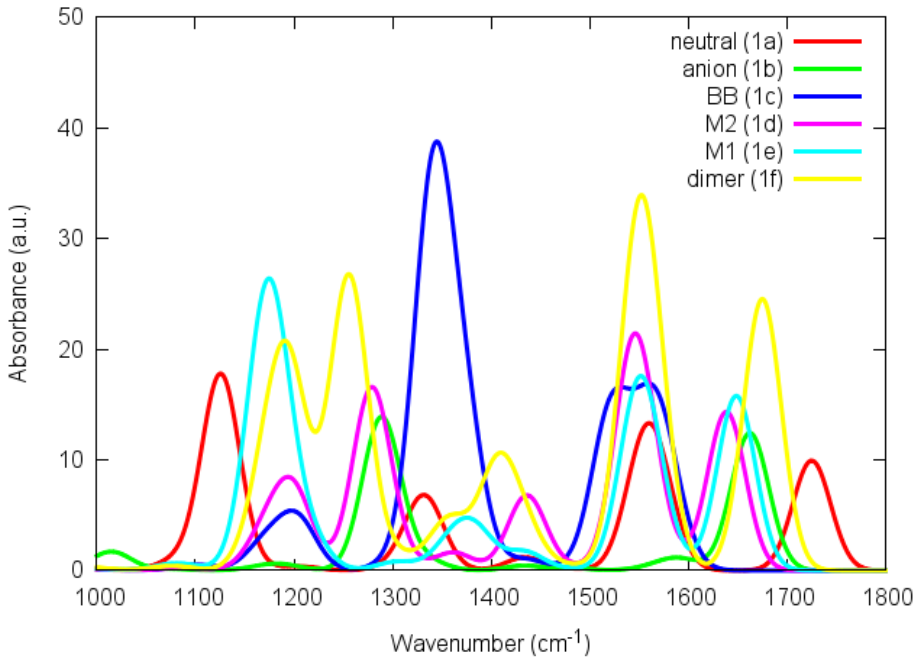


**Figure S3**. IR spectra computed at B3LYP/6-31G* in acetonitrile solution for system **1** in all anchoring environments modeled (structures **1a-1f** in Figure 4).

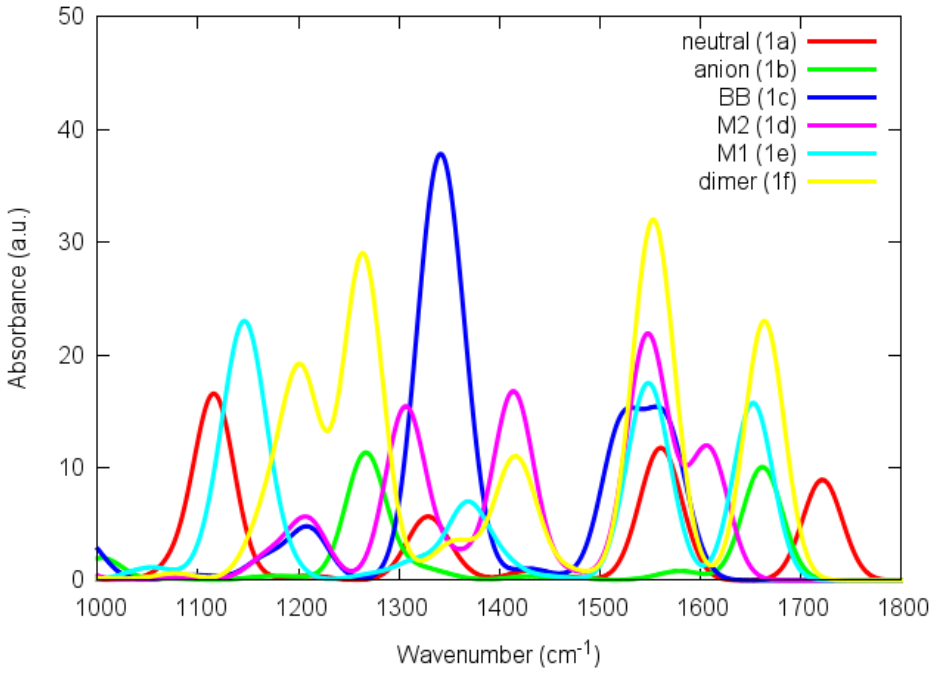


**Figure S4**. IR spectra computed at PBE0/6-31G* in acetonitrile solution for system **1** in all anchoring environments modeled (structures **1a-1f** in Figure 4).

**Table S1**. Bond distances (in Å) for the different models of **1** optimized at the B3LYP/6-31G* level.

| System | $Ti_1-O_1$ ($Ti_2-O_2$) | $C-O_1$ | $C-O_2$ | $O_2-H$ | $H\cdots O_{3/4}$ |
|---|---|---|---|---|---|
| **1a** | - | 1.214 | 1.35 | 0.975 | - |
| **1b** | - | 1.248 | 1.249 | - | - |
| **1c** | 2.093 (2.019) | 1.265 | 1.275 | - | 0.973 |
| **1d** | 2.300 | 1.243 | 1.311 | 1.012 | 1.626 |
| **1e** | 2.241 | 1.233 | 1.317 | 0.999 | 1.726 |
| **1f** | - | 1.233 | 1.319 | 1.000 | - |

**Table S2**. Infrared frequencies (in $cm^{-1}$) of the main vibrational modes present in a dye@semiconductor linkage and the $\Delta\nu_{as}$ value at the PBE0/6-31G* level of theory (gas phase).

| System | CO asymm | CO symm | C=C | C−H | $\Delta\nu_{as}$ |
|---|---|---|---|---|---|
| **1a** | 1740 | 1340 | 1570 | 1340 | 400 |
| **1b** | 1700 | 1240 | 1580 | 1320 | 460 |
| **1c** | 1540 | 1370 | 1580 | 1340 | 170 |
| **1d** | 1650 | 1440 | 1570 | 1350 | 200 |
| **1e** | 1660 | 1390 | 1560 | 1320 | 270 |
| **1f** | 1690 | 1420 | 1570 | 1350 | 270 |

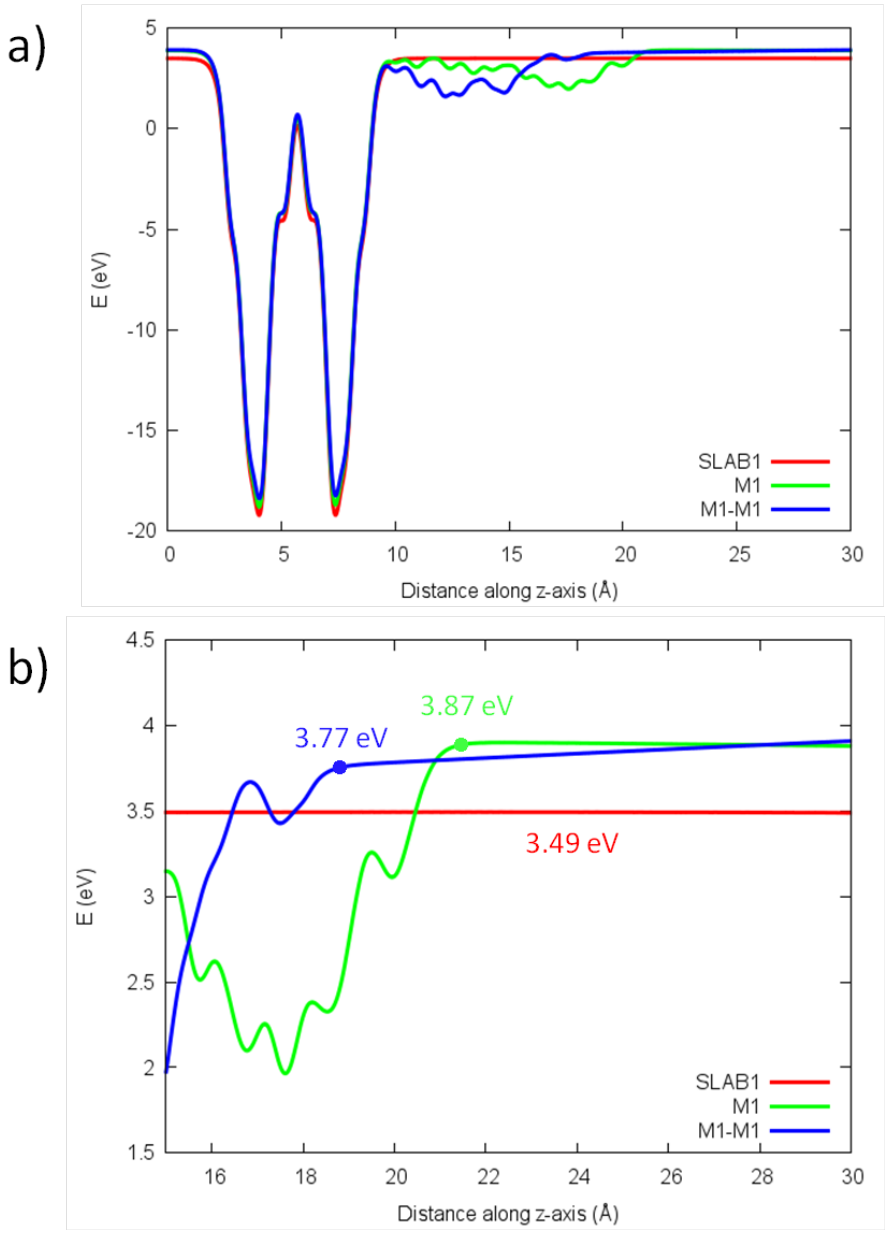


**Figure S5**. a) Electrostatic potential averages in the xy plane along the direction normal to the surface of the semiconductor (z) for the dye-sensitized $TiO_2$ SLAB1. b) Electrostatic potential averages in the region where the potential starts to behave linearly; values of vacuum level are determined at the point where the electrostatic potential profiles start to show this linear behavior.

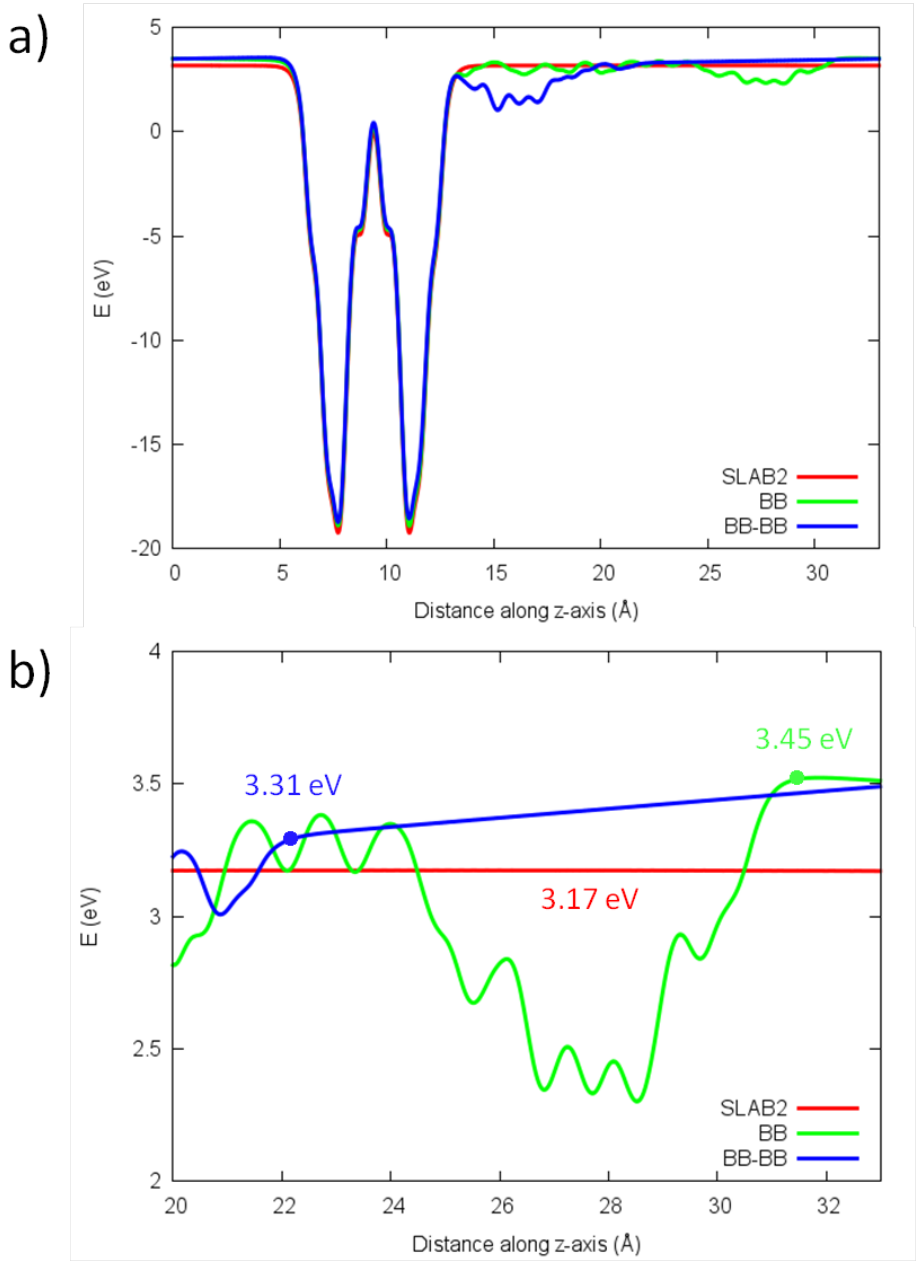


**Figure S6**. a) Electrostatic potential averages in the xy plane along the direction normal to the surface of the semiconductor (z) for the dye-sensitized $TiO_2$ SLAB2. b) Electrostatic potential averages in the region where the potential starts to behave linearly; values of vacuum level are determined at the point where the electrostatic potential profiles start to show this linear behavior.

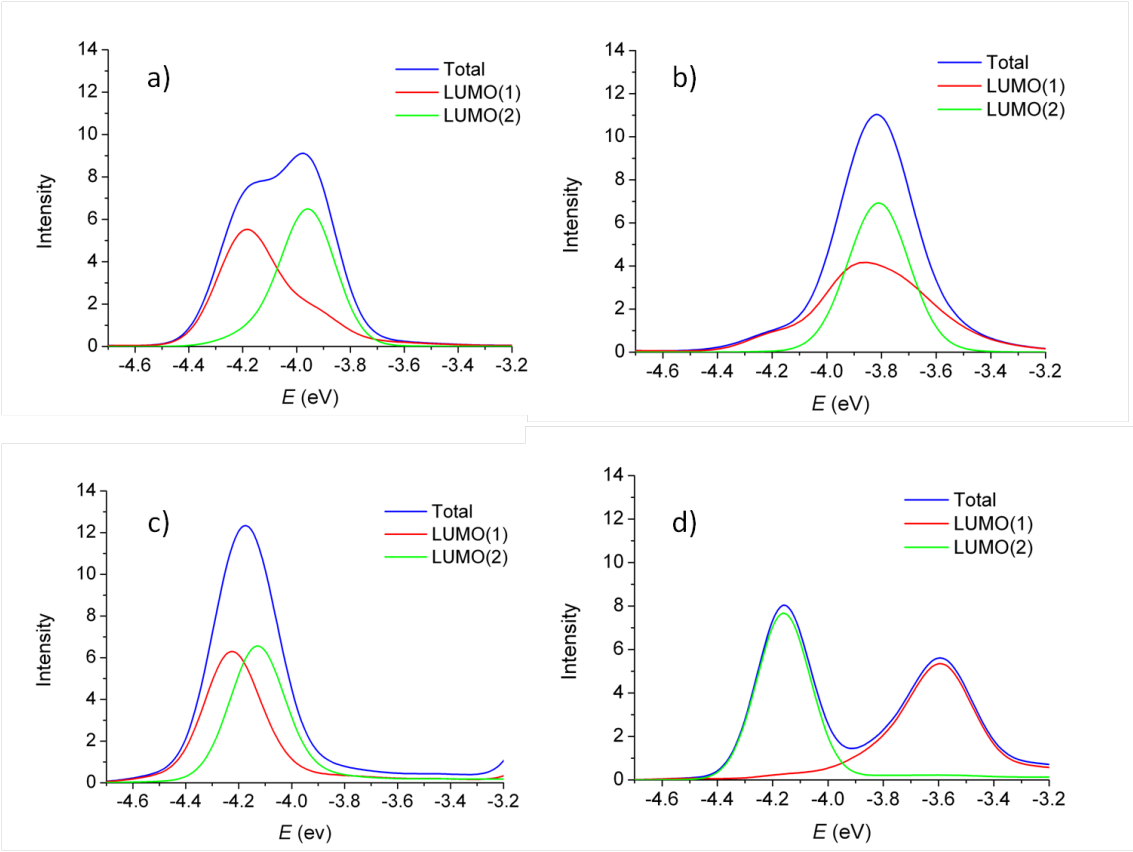


**Figure S7**. PDOS for the entire dye (total), the better-anchored branch LUMO(1) and the worse- or non-anchored branch LUMO(2) that contribute to the lowest unoccupied states in **2**@$TiO_2$ for the M1 (a), BB (b), M1-M1 (c) and BB-BB (d) absorption modes.